


# Stability restoration by asymmetric nonlinear states in non-Hermitian double-well potentials

Dmitry A. Zezyulin 

*School of Physics and Engineering, ITMO University, 197101 St. Petersburg, Russia  
and Abrikosov Center for Theoretical Physics, MIPT, Dolgoprudny, 141701 Moscow Region, Russia*



(Received 19 January 2024; accepted 21 March 2024; published 8 April 2024)

We introduce a class of one-dimensional complex optical potentials that feature a nonlinearity-induced stability restoration, i.e., the existence of stable nonlinear modes propagating in a waveguide whose linear eigenmodes are unstable. The optical potential is an even function of the transverse coordinate, i.e., the system is parity symmetric but not parity-time symmetric. The stability restoration occurs for asymmetric stationary nonlinear modes that do not respect the parity symmetry. Stable nonlinear states exist either for focusing and defocusing nonlinearities. On the qualitative level the stability restoration can be analyzed using a simple bimodal system. Its solutions enable systematic construction of stable stationary modes and more complex patterns with intensity periodically oscillating along the propagation distance.

DOI: [10.1103/PhysRevA.109.043510](https://doi.org/10.1103/PhysRevA.109.043510)

## I. INTRODUCTION

Ongoing progress in experimental realization of non-Hermitian optical systems [1–7] intensifies the discussions on the joint impact that non-Hermiticity and nonlinearity make on the existence and stability of guided waves. Either nonlinearity and non-Hermiticity make the propagation of light more intricate and are therefore expected to make the stability more fragile. In the meantime, a few remarkable situations are known where the nonlinearity makes the propagation of non-Hermitian waves more stable as compared to effectively linear states. A prominent development in this direction has been made by the proposal of the concept of nonlinearly induced parity-time ( $\mathcal{PT}$ ) symmetry transition [8] (see also [9]). For a class of periodic  $\mathcal{PT}$ -symmetric potentials, authors of Ref. [8] found that if the optical power is high enough, the Bloch spectrum of nonlinear waves can become purely real, even though the spectrum of propagation constants of linear waves is partially complex. A similar behavior was encountered for a class of bimodal  $\mathcal{PT}$ -symmetric systems [10–12], where the total power remained bounded (or even constant) along the propagation distance regardless of the value of the gain-loss coefficient. In a weaker sense, the stabilization by nonlinearity can be understood as the existence of dynamically stable nonlinear modes in a system whose linear waves (i.e., waves of infinitesimally small amplitude) are unstable. Using the language of spectral stability, in these systems the nonlinear potential suppresses eigenmodes that were unstable in the underlying linear limit. Situations of this type have been encountered multiple times in previous studies, either in finite-mode setups [13] and in spatially continuous waveguides [14–18]. Still, systematic studies of the nonlinearity-induced stabilization are scarce and mainly limited to  $\mathcal{PT}$ -symmetric systems.

The main goal of this paper is to introduce a nonlinearity-induced stability restoration in a continuous and non- $\mathcal{PT}$ -symmetric system. We consider light propagating in a parity-symmetric (but not parity-time symmetric) complex

potential whose real part has a double-well structure (or a double-hump structure if considered as an optical potential created by transversely varying refractive index). We show that in the linear regime the system cannot have stable localized guided modes, and instability of linear modes is protected by the parity symmetry of the potential. The degree of instability of linear waves is mediated by the distance between the potential wells. Most importantly, we find that nonlinearity suppresses the unstable eigenvalues and enables stable propagation of stationary states and periodically oscillating patterns. In a very unconventional manner, the nonlinearity-induced stabilization occurs for asymmetric stationary modes which do not respect the parity symmetry inherent to the system. Another important feature is that stabilization occurs for either sign (focusing and defocusing) of the optical nonlinearity.

The rest of the paper is organized as follows. In Sec. II we introduce our model and discuss its instability in the linear regime. Section III contains the main results on the existence of stable nonlinear patterns. In Sec. IV we summarize and discuss the outcomes of our study.

## II. THE MODEL AND ITS LINEAR PROPERTIES

We model the light propagation using the following dimensionless equation for complex-valued envelope of the electric field  $\Psi(x, z)$ :

$$i\Psi_z + \Psi_{xx} + [w^2(x) + iw_x(x)]\Psi + \sigma|\Psi|^2\Psi = 0. \quad (1)$$

In this nonlinear Schrödinger-type equation  $z$  and  $x$  stand for longitudinal and transverse coordinates, and  $\sigma$  is a coefficient of cubic Kerr nonlinearity. We consider both focusing ( $\sigma > 0$ ) and defocusing ( $\sigma < 0$ ) cases. Equation (1) incorporates an additional optical potential that describes the modulation of complex-valued refractive index in the transverse direction. The corresponding landscape is given by the term  $w^2(x) + iw_x(x)$ , where  $w(x)$  is a smooth real-valued function,  $w_x(x)$  is its derivative, and  $i$  is the imaginary unit. Potentials of this

form are sometimes referred to as Wadati potentials, after the author of Ref. [19] where their relevance was emphasized in the context of  $\mathcal{PT}$  symmetry.

To explain such a choice of the optical landscape, we note that potentials of this form have been already used to construct continuous families of nonlinear modes and solitons in  $\mathcal{PT}$ -symmetric and asymmetric non-Hermitian waveguides [20–25]. In the  $\mathcal{PT}$ -symmetric case [which corresponds to even functions  $w(x) = w(-x)$ ], Wadati potentials enable pitchfork  $\mathcal{PT}$ -symmetry-breaking bifurcations [26] that are unknown to occur in  $\mathcal{PT}$ -symmetric potentials of other shapes. Another important feature of Wadati potentials is that their linear eigenvalues are either real or exist in complex-conjugate pairs [27]. Therefore, similar to  $\mathcal{PT}$ -symmetric systems, Wadati potentials can undergo the phase transition from all-real to partially complex spectra [28,29]. A possibility of optical realization of Wadati potentials has been suggested for light propagating in a gas of coherent multilevel atoms driven by an external laser field [30].

Regarding the stability restoration discussed in this paper, it becomes possible due to special properties of Wadati potentials explained below. In contrast to most of previous studies dealing with Wadati potentials, we consider  $w(x)$  to be an antisymmetric (i.e., odd) function:

$$w(x) = -w(-x). \quad (2)$$

We also assume that  $w(x)$  and its derivative  $w_x(x)$  decay rapidly as  $x \rightarrow +\infty$  and  $x \rightarrow -\infty$ . For such a choice of function  $w(x)$ , the resulting optical potential  $w^2(x) + iw_x(x)$  is parity symmetric but *not* parity-time symmetric (nevertheless, as we will discuss below, its properties can be, in a certain sense, approximated by a  $\mathcal{PT}$ -symmetric model).

Our first result applies to the linear case [i.e.,  $\sigma = 0$  in Eq. (1)]. We argue that a linear waveguide with the potential introduced above can not guide localized eigenmodes with real propagation constants. Indeed, for stationary modes  $\Psi = e^{i\beta z}\psi(x)$ , Eq. (1) with  $\sigma = 0$  becomes a linear eigenvalue problem:

$$\beta\psi = \mathcal{L}\psi, \quad \mathcal{L} = \partial_x^2 + w^2(x) + iw_x(x), \quad (3)$$

where  $\beta$  is the propagation constant. Operator  $\mathcal{L}$  in Eq. (3) is a non-self-adjoint one-dimensional Schrödinger operator (precisely speaking,  $-\mathcal{L}$  is a Schrödinger operator). Since potential  $w^2(x) + iw_x(x)$  rapidly decays to zero, operator  $\mathcal{L}$  has a continuous spectrum which occupies the semiaxis  $\beta \in (-\infty, 0]$ . Operator  $\mathcal{L}$  can also have discrete eigenvalues associated with localized eigenfunctions  $\psi(x)$ . These eigenvalues (if any) are either positive real numbers or complex numbers. Due to the parity symmetry, any localized eigenfunction  $\psi(x)$  of operator  $\mathcal{L}$  in (3) is either even or odd function of  $x$ . On the other hand, from the properties of Wadati potentials it is known [27] that if  $\psi(x)$  is an eigenfunction corresponding to an eigenvalue  $\beta$ , then  $(\eta\psi(x))^*$ , where  $\eta = \partial_x + iw(x)$ , is an eigenfunction corresponding to eigenvalue  $\beta^*$  (the asterisk means complex conjugation). If  $\beta$  is real, then two eigenfunctions  $\psi$  and  $(\eta\psi(x))^*$  correspond to the same eigenvalue. However, it is well known that in one dimension the Schrödinger operator cannot have multiple eigenvalues with localized eigenfunctions [31]. Hence  $\psi$  and  $(\eta\psi(x))^*$  must be linearly dependent, which is impossible, because functions

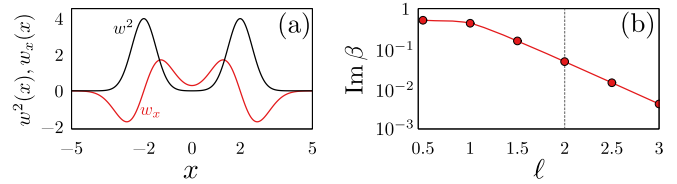


FIG. 1. (a) Real [ $w^2(x)$ ] and imaginary [ $w_x(x)$ ] parts of an optical potential generated by function (5) with  $W_0 = 2$  and  $\ell = 2$ . (b) Imaginary part of the unstable propagation constant for  $W_0 = 2$  and increasing well separation  $\ell$ .

$\psi(x)$  and  $\eta\psi(x)$  have opposite parities. Therefore, the propagation constant  $\beta$  cannot be real.

The same result can also be deduced from earlier literature. To this end, let us recall the well-known connection between Eq. (3) and the Zakharov-Shabat (ZS) spectral problem [32] that plays the central role in the inverse scattering theory for the modified Korteweg–de Vries equation [33]. Indeed, let us consider the ZS problem in the form

$$p_x = -i\zeta p + w(x)q, \quad q_x = i\zeta q - w(x)p, \quad (4)$$

for eigenvector  $(p(x), q(x))$  and eigenvalue  $\zeta$ . Then function  $\psi = q - ip$  satisfies Eq. (3) with  $\beta = -\zeta^2$  [33]; see also [1,20,21]. It is known that if  $w(x)$  decays to zero rapidly enough, then the continuous spectrum of the ZS problem fills the whole real axis  $\zeta \in \mathbb{R}$ . At the same time, the ZS problem can also have discrete eigenvalues  $\zeta$  that are always situated symmetrically with respect to the imaginary axis, i.e., if  $\zeta$  is an eigenvalue, then so is  $-\zeta^*$ . Guided modes with localized envelopes  $\psi(x)$  and real propagation constants  $\beta$  correspond to purely imaginary eigenvalues  $\zeta$  of the ZS problem. However, according to Theorem 3.4 in Ref. [34], if  $w(x)$  is an odd function, then the ZS problem has no purely imaginary eigenvalues.

As a side note, Wadati potentials  $w^2(x) + iw_x(x)$  are strongly reminiscent of the famous Miura transformation [35] that relates the Korteweg–de Vries equation and the modified Korteweg–de Vries equation.

We have established that for antisymmetric function  $w(x)$  the discrete spectrum of propagation constants is either empty or consists of one or several complex-conjugate pairs with eigenfunctions having opposite parities and being intertwined by operator  $\eta$ . In each complex-conjugate pair, one of the modes indefinitely grows along the propagation distance, which renders the linear waveguide unstable. Changing the sign of function  $w(x)$  complex conjugates the spectrum, i.e., attenuated and amplified modes swap.

In the rest of this paper we consider the situation where the real part of the optical potential has a double-lobe structure. A representative example of suitable odd function  $w(x)$  is

$$w(x) = W_0 e^{-(x-\ell)^2} - W_0 e^{-(x+\ell)^2}, \quad (5)$$

where  $W_0$  is the amplitude and  $\ell$  is the half-distance between the lobes [see plot in Fig. 1(a)]. As the half-distance  $\ell$  increases, the complex-conjugate propagation constants become closer to the real axis, i.e., the instability weakens [see Fig. 1(b)]. For sufficiently large  $\ell$  the decay of imaginary parts is nearly exponential. Our main result demonstrates that

even in the regime where the instability increment of the linear propagation constant is not yet very small, the nonlinearity enables propagation of stable modes.

### III. MAIN RESULTS

#### A. Two-mode system

We consider the situation where the linear operator  $\mathcal{L}$  in Eq. (3) has exactly two discrete propagation constants which are denoted as  $\beta_{\pm}$ . According to the above analysis, these values must be complex conjugate:  $\beta_+ = \beta_-^*$ . We denote the corresponding eigenfunctions as  $\psi_{\pm}(x)$  and normalize them such that  $\int_{-\infty}^{\infty} |\psi_{\pm}(x)|^2 dx = 1$ . As explained above, these functions have opposite parities and are therefore orthogonal:  $\int_{-\infty}^{\infty} \psi_+^*(x) \psi_-(x) dx = 0$ . This distinguishes our analysis from the  $\mathcal{PT}$ -symmetric case, where the eigenfunctions associated with different eigenvalues are generically not orthogonal in the usual sense.

We further assume that phases of eigenfunctions  $\psi_{\pm}(x)$  are chosen such that the following linear combinations correspond to the superpositions localized in the right ( $R$ ) and left ( $L$ ) wells:

$$\varphi_{R,L}(x) = [\psi_+(x) \pm \psi_-(x)]/\sqrt{2}. \quad (6)$$

These functions are normalized and orthogonal too:  $\int_{-\infty}^{\infty} \varphi_R^*(x) \varphi_L(x) dx = 0$ ,  $\int_{-\infty}^{\infty} |\varphi_{R,L}(x)|^2 dx = 1$ . We introduce a pair of real constants

$$b = \frac{\beta_+ + \beta_-}{2}, \quad \gamma = \frac{\beta_- - \beta_+}{2i}. \quad (7)$$

Without loss of generality  $\gamma > 0$ . We look for solutions of Eq. (1) in the form of a two-mode substitution

$$\Psi(x, z) = e^{ibz} [a_R(z) \varphi_R(x) + a_L(z) \varphi_L(x)]. \quad (8)$$

If the separation between the well (respectively, humps) of the potential is large enough, i.e.,  $2\ell \gg 1$  in Eq. (5), then the integrals containing the cross products between  $\varphi_R$  and  $\varphi_L$  can be assumed negligible, and one can approximate the evolution of the envelope  $\Psi(x, z)$  by the following coupled-mode system:

$$\begin{aligned} i\dot{a}_R &= i\gamma a_L - \chi |a_R|^2 a_R, \\ i\dot{a}_L &= i\gamma a_R - \chi |a_L|^2 a_L, \end{aligned} \quad (9)$$

where overdots mean derivatives with respect to  $z$ , and  $\chi = \sigma \int_{-\infty}^{\infty} |\varphi_R|^4 dx = \sigma \int_{-\infty}^{\infty} |\varphi_L|^4 dx$ .

Even though system (9) is obtained using the standard two-mode approach, it differs dramatically from the previously considered systems describing bosonic Josephson oscillations in real double-well potentials (see, e.g., [36,37]) due to the imaginary unit in the coupling terms. This change renders the dynamics non-Hermitian. In particular, the imbalance between the right and left amplitudes is conserved:

$$\partial_z (|a_R|^2 - |a_L|^2) = 0. \quad (10)$$

This is in a stark contrast to the periodic tunneling between the left and right subsystems typical of usual double-well (or double-lobe) potentials.

In the linear case (that is for  $\chi = 0$ ), the general solution of system (9) is

$$\begin{pmatrix} a_R \\ a_L \end{pmatrix} = \alpha_1 e^{\gamma z} \begin{pmatrix} 1 \\ 1 \end{pmatrix} + \alpha_2 e^{-\gamma z} \begin{pmatrix} 1 \\ -1 \end{pmatrix}, \quad (11)$$

where  $\alpha_{1,2}$  are constants. The solution corresponding to the growing exponent  $e^{\gamma z}$  blows up to infinity as  $z \rightarrow \infty$ . Therefore, the zero equilibrium  $(a_R, a_L) = (0, 0)$  is an unstable fixed point of the nonlinear system (9).

After a simple transformation, the coupled-mode system (9) can be brought to the form of a  $\mathcal{PT}$ -symmetric nonlinearly coupled dimer. Representing  $a_R = u + v$ ,  $a_L = u - v$ , where  $u$  and  $v$  are new functions, from system (9) we obtain

$$\begin{aligned} i\dot{u} &= i\gamma u - \chi [(|u|^2 + 2|v|^2)u + v^2 u^*], \\ i\dot{v} &= -i\gamma v - \chi [(|v|^2 + 2|u|^2)v + u^2 v^*]. \end{aligned} \quad (12)$$

A very similar (yet not fully identical) dynamical system has been earlier considered in [10] as an exactly solvable  $\mathcal{PT}$ -symmetric dimer. For that system the authors of Ref. [10] found that the nonlinearity ‘softens’ the  $\mathcal{PT}$  phase transition, i.e., stable nonlinear states can be found for arbitrarily large non-Hermiticity coefficient  $\gamma$ , provided that the solution amplitude is large enough. In contrast to our system in Eqs. (12), the  $\mathcal{PT}$ -symmetric dimer considered in Ref. [10] contained additional linear coupling, i.e., terms  $\kappa v$  and  $\kappa u$  in the first and second equations, respectively, where  $\kappa > 0$  was the coupling coefficient. In our system, that linear coupling is absent. This difference leads to a moderate modification of our two-mode analysis as compared to that developed in Ref. [10].

Dynamics of the bimodal system (9) can be analyzed in terms of the Stokes parameters defined as

$$\{X, Y, Z\} = (a_R^*, a_L^*) \sigma_{\{x,y,z\}} (a_R, a_L)^T, \quad (13)$$

where  $\sigma_{x,y,z}$  are the Pauli matrices, and superscript  $T$  means transposition. In those variables system (9) transforms into

$$\begin{aligned} \dot{X} &= 2\gamma A + \chi YZ, \\ \dot{Y} &= -\chi XZ, \\ \dot{Z} &= 0. \end{aligned} \quad (14)$$

These equations additionally involve the length of the Stokes vector  $A$  which characterizes the total energy stored in both modes:

$$A = (X^2 + Y^2 + Z^2)^{1/2} = |a_R|^2 + |a_L|^2. \quad (15)$$

Its dynamics obeys the following equation:

$$\dot{A} = 2\gamma X. \quad (16)$$

Equations (14) and (16) can be combined into a simple linear equation

$$\ddot{X} + v^2 X = 0, \quad (17)$$

where we have introduced

$$v^2 = (\chi Z)^2 - 4\gamma^2. \quad (18)$$

Bounded orbits are possible only if the condition  $v^2 > 0$  is satisfied, that is for  $|\chi Z| > 2\gamma$ . Since the Stokes parameter  $Z = |a_R|^2 - |a_L|^2$  corresponds to the imbalance between the amplitudes of right and left modes, we conclude that, in terms

of the starting Eq. (1), any stable solution (if exists at all) *must* be asymmetric with respect to the parity reversal:  $|\Psi(x, z)| \neq |\Psi(-x, z)|$ .

Equations (14) and (16) are fully solvable [10]. For  $\nu^2 > 0$  the general solution reads as

$$X(z) = \rho_0 \cos \phi, \quad (19)$$

$$Y(z) = \frac{-1}{\nu} [2\gamma \sqrt{Z^2 + \rho_0^2} \operatorname{sgn}(\chi Z) + \chi Z \rho_0 \sin \phi], \quad (20)$$

$$Z = \text{const}, \quad (21)$$

where  $\phi = \nu(z - z_0)$ , and  $z_0$  and  $\rho_0$  are arbitrary constants of integration. The value of the conserved quantity  $Z$  is arbitrary too, provided that inequality  $\nu^2 > 0$  holds. For the length of the Stokes vector  $A$  we compute

$$A(z) = \frac{1}{\nu} [\sqrt{Z^2 + \rho_0^2} |\chi Z| + 2\gamma \rho_0 \sin \phi]. \quad (22)$$

If  $\nu^2 < 0$ , all nontrivial solutions of equations (14) and (16) grow indefinitely as  $z \rightarrow +\infty$ . We do not consider this case.

### B. Fixed points of the two-mode system

The conserved quantity  $Z$  can be used to parametrize found solutions in the phase space  $(X, Y, Z)$ . Any motion is restricted to the plane  $Z = \text{const}$ , and every solution  $(X(z), Y(z))$  given by Eqs. (19) and (20) forms an ellipse in the corresponding  $Z$  plane. Moreover, each plane  $Z = \text{const}$  is filled by nested ellipses that correspond to different values of the integration constant  $\rho_0$  in Eqs. (19) and (20). Each plane  $Z = \text{const}$  contains exactly one fixed point which can be found by setting  $\rho_0 = 0$ :

$$X_0 = 0, \quad Y_0 = -2\nu^{-1}\gamma Z \operatorname{sgn} \chi, \quad A_0 = \nu^{-1} |\chi| Z^2. \quad (23)$$

Hereafter, we use subscript 0 to distinguish values of Stokes parameters  $X$ ,  $Y$ , and  $A$  that pertain to fixed points. This fixed point lies inside all nested ellipses hosted in the corresponding  $Z$  plane and is therefore stable. Each fixed point corresponds to a solution of the form  $a_R(z) = U_R e^{i\omega z}$ ,  $a_L(z) = U_L e^{i\omega z - i\alpha}$ , where  $U_{R,L}$ ,  $\alpha$ , and  $\omega$  are real constants. Value of  $\omega$  can be retrieved from the two-mode system (9):

$$\omega = \chi \frac{A_0^2 + Z^2}{2A_0} = \operatorname{sgn} \chi \frac{\chi^2 Z^2 - 2\gamma^2}{\sqrt{\chi^2 Z^2 - 4\gamma^2}}. \quad (24)$$

Parameter  $\omega$  is physically relevant because it gives the distance between the propagation constant  $\beta$  of a nonlinear mode and the point where the linear modes are situated, i.e., from  $b = (\beta_+ + \beta_-)/2$  [see Eqs. (7) and (8)]:

$$\beta = b + \omega. \quad (25)$$

It is therefore natural to scan Eq. (24) for different  $\omega$  and solve it with respect to  $Z$ . Simple analysis shows that Eq. (24), considered as an equation with respect to  $Z$ , has real roots if and only if

$$\operatorname{sgn} \omega = \operatorname{sgn} \chi \quad \text{and} \quad |\omega| \geq \omega_C := 2\sqrt{2}\gamma, \quad (26)$$

where subscript ‘‘C’’ refers to points  $C_{\pm}$  in Fig. 2 (see discussion below). If conditions (26) hold, then all solutions are

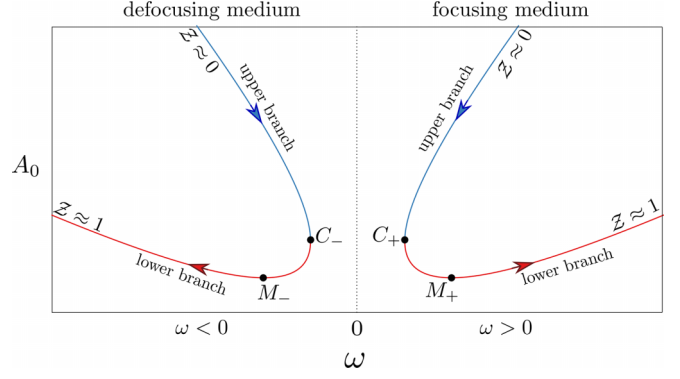


FIG. 2. Schematic diagram of fixed points of the two-mode system (9) displayed as dependencies  $A_0(\omega)$  in focusing and defocusing media. In terms of the full system, quantities  $A_0$  and  $\omega$  transform in squared norm and propagation constant of stationary nonlinear modes, respectively; compare this figure with Fig. 3 which shows analogous dependencies produced from full envelope Eq. (1). Arrows show directions which correspond to the increase of the normalized asymmetry parameter  $Z$  from its asymptotic minimal value  $Z = 0$  up to the maximal asymptotic value  $Z = 1$ . Labels  $C_{\pm}$  mark the points where the upper and the lower subbranches meet pairwise. Labels  $M_{\pm}$  mark the points where the minimal values of  $A_0$  are achieved.

given as

$$Z = \pm \frac{1}{\sqrt{2}|\chi|} \sqrt{\omega^2 + 4\gamma^2 \pm |\omega| \sqrt{\omega^2 - \omega_C^2}}, \quad (27)$$

where all four combinations of signs  $+$  and  $-$  are possible. If  $|\omega|$  is strictly larger than the critical value  $\omega_C$ , then there are four different solutions. In fact, the analysis can be limited only to two positive roots  $Z$  because negative  $Z$  correspond to the parity reversal  $a_R \leftrightarrow a_L$ .

In terms of the full model (1), Eq. (27) predicts that stable asymmetric nonlinear modes emerge as the propagation constant  $\beta$  gets far enough from the point  $b$ , where the unstable linear modes are situated. The critical difference between  $\beta$  and  $b$  is given by  $\pm\omega_C$ ; this difference must be positive (negative) for focusing (defocusing) nonlinearity. It also readily follows from (27) that for either sign of nonlinearity, two physically distinct nonlinear solutions are born simultaneously at a foldlike bifurcation corresponding to  $\omega = \pm\omega_C$ .

Equations (23) and (27) provide all the necessary information to compute all Stokes parameters corresponding to the fixed points and trace their dependence on the propagation constants mismatch  $\omega$ . In Fig. 2 we show a representative schematics that illustrates the behavior of the Stokes parameters on the plane  $A_0$  vs  $\omega$ . We choose these parameters to display because they can be easily transformed to physically relevant squared norm and propagation constant of nonlinear modes. Indeed, if  $\Psi(x, z) = e^{i\beta z} \psi(x)$  is a stationary nonlinear mode, then the two-mode substitution (8) implies that  $\int_{-\infty}^{\infty} |\psi(x)|^2 dx = A_0$  and  $\beta = \omega + b$  [see Eq. (25)]. The diagram in Fig. 2 presents two curves: one for a focusing and another one for a defocusing medium, and each curve consists of two subbranches (upper branch and lower branch) which merge pairwise exactly at  $\omega = \pm\omega_C$ , where  $\omega_C$  is the threshold value defined in (26). In Fig. 2, we use labels  $C_{\pm}$



to highlight the points where solutions from upper and lower subbranches meet pairwise:

$$C_{\pm} : A_{0,C} = \frac{3\sqrt{2}\gamma}{|\chi|}, \quad \omega_{C_{\pm}} = \pm 2\sqrt{2}\gamma. \quad (28)$$

The diagram in Fig. 2 also contains two other special points denoted as  $M_{\pm}$ . They correspond to the minimal possible value of  $A_0$ :

$$M_{\pm} : A_{0,M} = \frac{4\gamma}{|\chi|}, \quad \omega_{M_{\pm}} = \pm 3\gamma. \quad (29)$$

This result is natural: the larger the increment of instability of linear waves  $\gamma$ , the larger norm  $A_{0,M}$  is necessary for nonlinear modes to overcome the instability of linear waves and get born; in a similar way, the larger mismatch is necessary between propagation constants of nonlinear and linear modes.

In Fig. 2 we also illustrate the behavior of the normalized asymmetry parameter  $\mathcal{Z}$  defined as

$$\mathcal{Z} = \frac{Z}{A_0} = \frac{|a_R|^2 - |a_L|^2}{|a_R|^2 + |a_L|^2}. \quad (30)$$

Simple calculation gives the dependence of the normalized asymmetry measure  $\mathcal{Z}$  on  $A_0$ :

$$\mathcal{Z}^2 = \frac{1}{2} \left( 1 \mp \sqrt{1 - \frac{A_{0,M}^2}{A_0^2}} \right), \quad (31)$$

where  $A_{0,M}$  is the minimal value of  $A_0$  which is defined in (29). Here the minus sign corresponds to  $A_0$  decreasing from  $+\infty$  down to its minimal possible value  $A_{0,M}$ , and, respectively,  $\mathcal{Z}$  increasing from 0 up to  $1/\sqrt{2}$ . The plus sign corresponds to  $A_0$  increasing from  $A_{0,M}$  up to  $+\infty$ , and, respectively,  $\mathcal{Z}$  further increasing from  $1/\sqrt{2}$  up to its asymptotic maximal value equal to unity. In Fig. 2 we use arrows to indicate the directions along the plotted curves that correspond to the increase of asymmetry parameter  $\mathcal{Z}$ . Since  $\mathcal{Z}$  is different from zero for all solutions, we conclude that either upper and lower subbranches consist of asymmetric modes, that is  $|\psi(x)| \neq |\psi(-x)|$  for all stationary envelopes  $\psi$ . At the same time, the modes that correspond to lower subbranches are more asymmetric because the corresponding asymmetry parameter  $\mathcal{Z}$  is larger as compared to upper subbranches.

Apart from the fixed-point stationary solutions, two-mode system (9) predicts a variety of stable closed orbits which, in terms of full Eq. (1), correspond to localized modes whose intensity  $|\Psi(x, z)|$  changes periodically along the propagation distance.

### C. Stability restoration in the full equation

To check the predictions obtained from the simple two-mode system, we have computed stationary states of full Eq. (1). These have been sought in the form  $\Psi(x, z) = e^{i\beta z}\psi(x)$ , where  $\beta$  is real propagation constant and  $\psi(x)$  is stationary envelope. Numerical search of stationary states has been performed using a modified shooting approach adapted for peculiar properties of Wadati potentials [21,25]. The main results are presented in Fig. 3 as dependencies of the energy flow (or squared norm)  $U = \int_{-\infty}^{\infty} |\psi(x)|^2 dx$  on the propagation constant  $\beta$ . In the same figure we plot the analogous

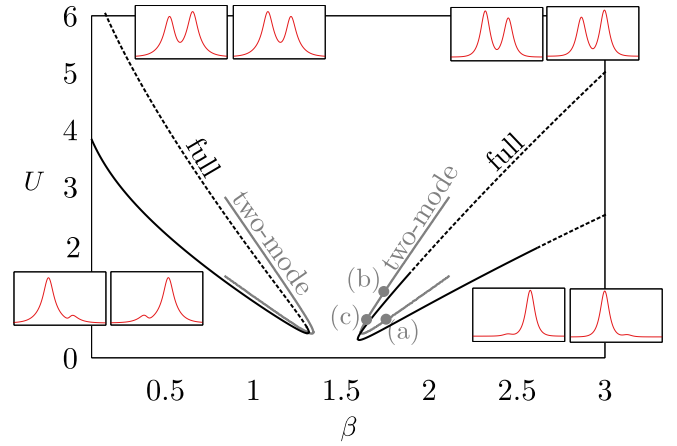


FIG. 3. Families of stationary nonlinear modes of full Eq. (1) (black curves) on the plane  $(U, \beta)$ , where  $U$  is the energy flow and  $\beta$  is the propagation constant, juxtaposed with the analogous dependencies obtained from the fixed points of the two-mode system (gray curves). Solid and dashed segments of curves for the full equation correspond to stable and unstable stationary modes, respectively. Small panels next to the energy flow curves illustrate schematically spatial shapes of nonlinear modes  $|\psi|$  at the corresponding subbranches: weakly and strongly asymmetric states are situated at the upper and lower subbranches, respectively. Points (a)–(c) at the two-mode curves in the focusing medium correspond to solutions used for dynamical simulations in Fig. 6. This figure is obtained for potential given by (5) with  $W_0 = 2$  and  $\ell = 2$ . Nonlinear modes obtained for focusing ( $\sigma = 1$ ) and defocusing ( $\sigma = -1$ ) nonlinearities are displayed simultaneously.

dependencies computed from fixed points of the two-mode system. We observe a reasonably good qualitative agreement between the results produced from the full equation and from the two-mode reduction. As the power flow becomes large enough, families of stationary modes get born in either focusing and defocusing media through foldlike bifurcations. It should be stressed that localized modes with real propagation constants form continuous families on the plane  $(U, \beta)$ : this is a special feature of Wadati [21] and  $\mathcal{PT}$ -symmetric [38] potentials as compared to complex-valued potentials of other shapes.

As the power flow  $U$  increases, the quantitative agreement between the analytical and numerical  $U(\beta)$  curves becomes worse. This is not surprising because the two-mode analysis uses the linear eigenfunctions as a basis to represent the nonlinear solution. Due to the growth of discrepancy, we display only lower parts of the analytical curves for nonlinear families in Fig. 3.

All fixed points of the bimodal system are stable. However, this does not yet guarantee that corresponding nonlinear modes of the full equation are stable too. We have therefore performed a numerical stability check for stationary solutions of Eq. (1). It proceeds in a standard way by considering a perturbed envelope  $\Psi(x, z) = e^{i\beta z}[\psi(x) + u(x)e^{i\lambda z} + v^*(x)e^{-i\lambda^*z}]$ , linearizing Eq. (1) with respect to small perturbations  $u, v$ , and computing the instability increments given by imaginary parts of eigenvalues  $\lambda$ . Fragments of energy flow curves that contain stable and unstable solutions are shown, respectively, with solid and dotted lines in Fig. 3.

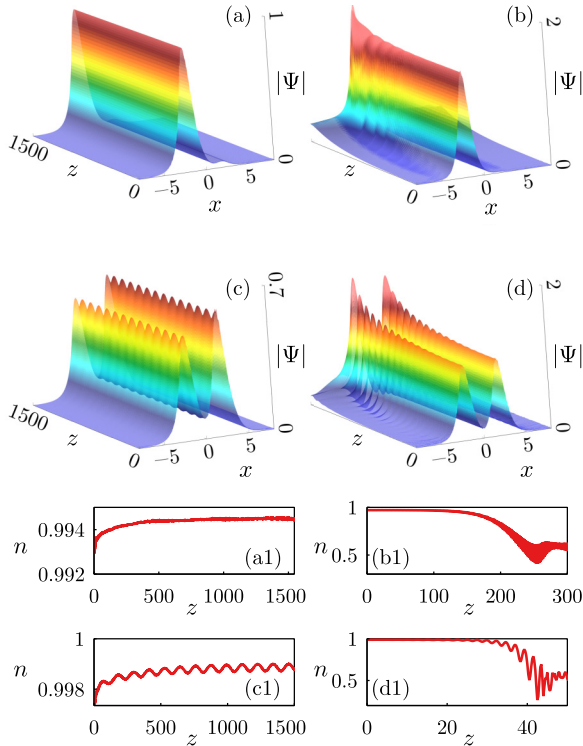


FIG. 4. Dynamical solutions of full Eq. (1) for initial conditions obtained from slightly perturbed stationary modes  $\psi(x)$  with relative perturbation amplitude  $\eta = 0.01$ , under the focusing nonlinearity with  $\sigma = 1$ : (a) lower subbranch,  $\beta = 2$  (stable); (b) lower subbranch,  $\beta = 3$  (unstable); (c) upper subbranch,  $\beta = 1.7$  (stable); (d) upper subbranch,  $\beta = 2.3$  (unstable). Four lower panels (a1)–(d1) display the corresponding dependencies  $n(z)$ , i.e., the energy-flow fraction stored in both left and right modes as defined by Eq. (32).

We observe that in the focusing medium both subbranches are stable close to the foldlike bifurcation, but become unstable for sufficiently large energy flow  $U$ . In the defocusing medium the lower (i.e., the strongly asymmetric) subbranch is totally stable while the upper one is unstable. Therefore, even though the linear modes of the system are unstable, the stability restoration takes place for asymmetric nonlinear modes in both focusing and defocusing media.

#### D. Dynamics of nonlinear modes

Examples of nonlinear dynamics computed from Eq. (1) with initial conditions taken in the form of stationary modes perturbed by a small-amplitude noise are shown in Fig. 4 (this figure corresponds to the focusing nonlinearity). In presented simulations, the numerical stationary envelope  $\{\psi_j\}$  computed on the finite grid  $\{x_j\}$ ,  $j = 1, \dots, N$ , was perturbed by replacing  $\psi_j$  with  $[1 + \eta(r_j + is_j)]\psi_j$ , where  $0 < \eta \ll 1$  is small relative amplitude, and sequences  $\{r_j\}$  and  $\{s_j\}$  were generated as vectors of pseudorandom numbers drawn from the standard normal distribution. In each case the dynamical behavior agrees with the linear stability prediction. In the same Fig. 4 we additionally show fraction of the energy stored in the left and right eigenfunctions which is computed as

$$n(z) = [|\tilde{a}_L(z)|^2 + |\tilde{a}_R(z)|^2]/U(z), \quad (32)$$

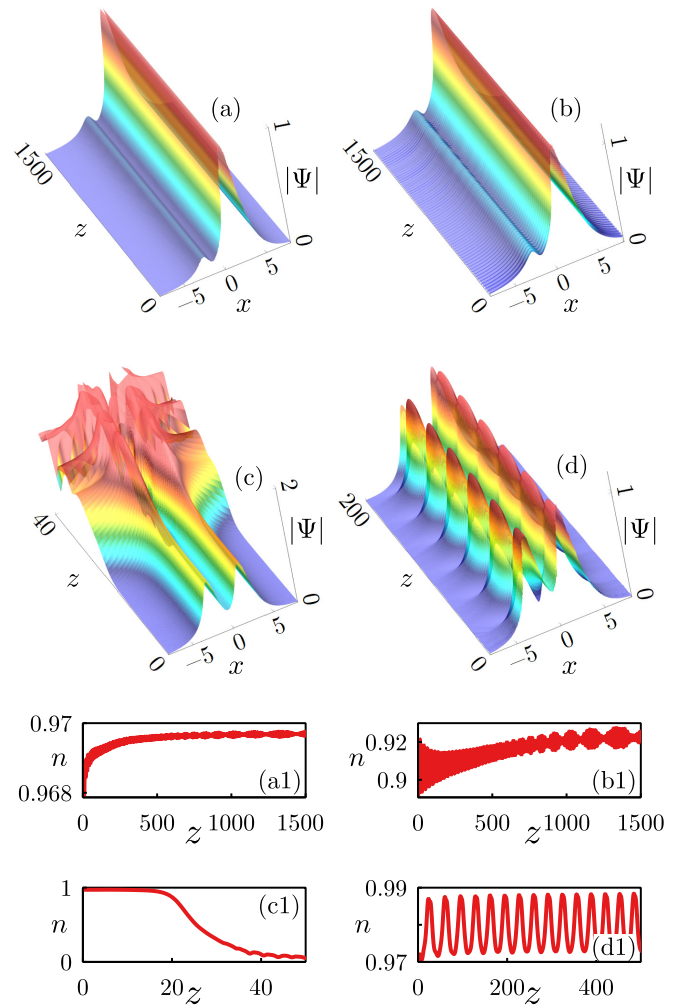


FIG. 5. Dynamical solutions of full Eq. (1) for initial conditions obtained from slightly perturbed stationary modes  $\psi(x)$  with relative perturbation amplitude  $\eta = 0.01$ , under the defocusing nonlinearity with  $\sigma = -1$ : (a), (b) lower subbranch,  $\beta = 0.6$  and  $0.2$  (both stable); (c), (d) upper subbranch  $\beta = 0.6$  for perturbation with  $\eta = 0.01$  (c) and  $\eta = 0.025$  and  $5\%$  (d). Four lower panels (a1)–(d1) display the corresponding dependencies of the energy-flow fraction stored in left and right modes as defined by Eq. (32).

where  $U(z) = \int_{-\infty}^{\infty} |\Psi(x, z)|^2 dz$  is the total energy flow, and coefficients  $\tilde{a}_{L,R}$  are obtained by projecting the solution onto the right and left states:

$$\tilde{a}_{R,L}(z) = \int_{-\infty}^{\infty} \Psi^*(x, z) \varphi_{R,L}(x) dx. \quad (33)$$

By definition,  $0 \leq n(z) \leq 1$ , and  $n = 1$  corresponds to the situation when the total energy flow is perfectly stored in the two modes. For stable evolutions in Fig. 4, we observe that  $n(z)$  remains close to unity, while unstable dynamics is accompanied by excitation of modes that are not taken into account by the reduced model.

Examples of stable and unstable dynamics for stationary modes under the defocusing nonlinearity are shown in Fig. 5. In accordance with the linear stability predictions, solutions from the lower subbranch are stable, while those from the upper subbranch are unstable. We have found that behavior of

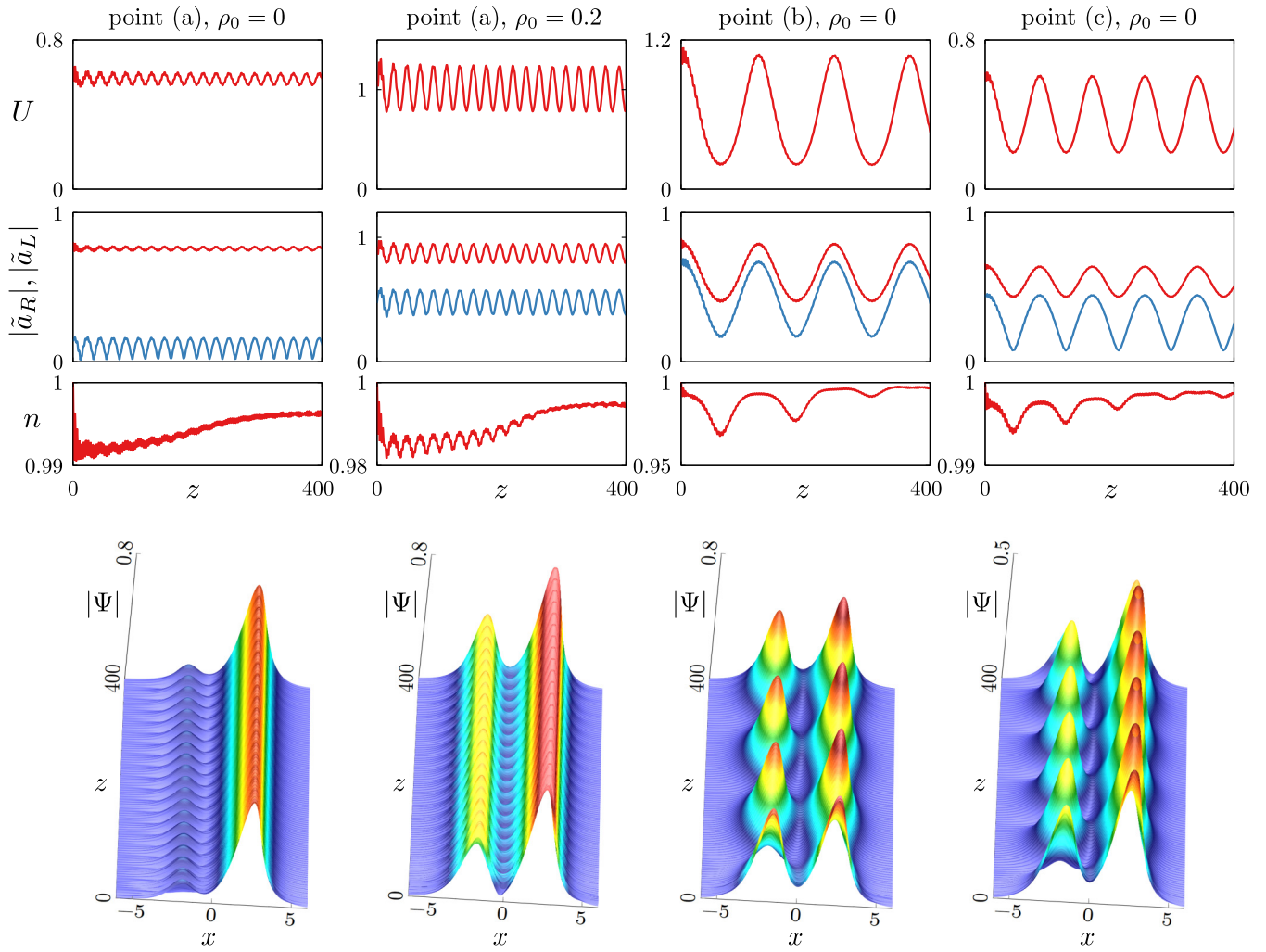


FIG. 6. Examples of evolutions computed from full Eq. (1) with initial data obtained as fixed points ( $\rho_0 = 0$ ) and periodic orbits ( $\rho_0 \neq 0$ ) of the two-mode reduction. Panels in the first, second, and third rows show the energy flow  $U(z) = \int_{-\infty}^{\infty} |\Psi(x, z)|^2 dx$ , amplitudes  $|\tilde{a}_{R,L}(z)|$  of projections of the solution  $\Psi(x, z)$  onto the left and right eigenmodes [see Eq. (33)], and the fraction of the energy conserved in the two modes  $n(z)$  defined in Eq. (32). Points (a)–(c) referred to in the upper row correspond to those labeled in Fig. 3. Full dynamical plots are shown in the bottom row. (b) This figure corresponds to the focusing nonlinearity.

unstable modes can be sensitive to the initial perturbation: for different amplitudes of random noise perturbed initial conditions can feature extreme broadening [Fig. 5(c)] or transform to an oscillating state [Fig. 5(d)]. In the latter case the fraction of energy stored in the left and right modes remains close to unity [Fig. 5(d1)]. This indicates that a perturbed unstable stationary mode dynamically transforms into a stable solution corresponding to a closed orbit in the reduced bimodal system.

### E. Periodic dynamics from the two-mode approximation

The two-mode approximation developed above can also be used for systematic generation of initial conditions that feature nontrivial dynamics in the full equation. We illustrate this result using three points labeled as (a)–(c) in Fig. 3: point (a) belongs to the lower subbranch of the two-mode curve, and points (b) and (c) belong to the upper subbranch. We use the corresponding fixed points and periodic orbits of the reduced two-mode system to prepare initial conditions for full Eq. (1).

The results are shown in Fig. 6 as dependencies of the energy flow  $U(z)$  (upper row), amplitudes  $|\tilde{a}_{R,L}(z)|$  of projections of the solution onto the right and left states [see the definition in (33)], and the fraction of energy stored in the two modes defined in (32).

We start with point (a) and use the initial conditions corresponding to a fixed point. In terms of the two-mode solution this corresponds to the zero integration constant:  $\rho_0 = 0$ . The energy flow and coefficients  $\tilde{a}_{R,L}$  computed from the full numerical solution (and shown in the first column of Fig. 6) feature oscillations of relatively small amplitude and therefore agree well enough with the predictions of the two-mode system (since the considered initial conditions correspond to the fixed point, the two-mode system obviously predicts that the plotted dependencies must be constant). Further, we increase the integration constant by taking  $\rho_0 = 0.2$ . In terms of the two-mode system this choice corresponds to a periodic orbit. The numerical solution obtained from the corresponding initial data (and shown in the second column of Fig. 6)

indeed features more appreciable oscillations than the previous solution. However for points (b) and (c) presented in third and fourth columns of Fig. 6 we observe that initial conditions corresponding to fixed points with  $\rho_0 = 0$  develop in full solutions with strong oscillations: in other words, instead of stationary modes corresponding to fixed points we excite solutions whose amplitudes  $|\Psi(x, z)|$  periodically change along the propagation distance. Even though these dynamics disagree with the predictions of the bimodal reduction, the latter still remains useful, for it enables systematic preparation of initial conditions that develop in stable periodic solutions of full Eq. (1). Oscillations of  $\tilde{a}_{R,L}(z)$  obtained from numerical solutions  $\Psi(x, z)$  are always in phase, which agrees with the prediction of the reduced system. We additionally note that for all data presented in Fig. 6 the energy flow is almost perfectly stored in left and right modes with  $n(t) \geq 0.96$ .

#### IV. CONCLUSION

We have demonstrated a phenomenon of nonlinearity-induced stabilization for a class of non-Hermitian optical potentials whose real part has a double-lobe structure. In contrast to most of the previous studies where a similar behavior has been encountered, our system is parity symmetric but not parity-time symmetric. Another salient difference from earlier results is that the stabilization occurs for asymmetric nonlinear states that do not respect the parity symmetry inherent to the potential. Moreover, the stabilization takes place for either sign of cubic nonlinearity. Analysis of the stability restoration has been developed using a simple two-mode system obtained by projecting the solution onto superpositions of linear eigenmodes centered in right and left wells of the potential. Dynamical simulations of full envelope equation confirm the existence of stable nonlinear modes and reveal the ubiquity of oscillating patterns with intensity periodically changing along the propagation distance. In contrast to familiar oscillations in double-well potentials that are most usually accompanied by

the tunneling between the wells, periodic patterns that we observe feature distinctively different behavior with the energies stored in the left and in the right wells oscillating in phase.

Our results have been obtained for a special class of complex potentials that correspond to the form  $w^2(x) + iw_x(x)$ , where  $w(x)$  is a real-valued and antisymmetric function and  $w_x(x)$  is its derivative. In a real-world system the optical landscape will never perfectly match this shape, and the propagation of light will be governed by a perturbed potential  $w^2(x) + iw_x(x) + \varepsilon r(x)$ , where  $r(x)$  describes a complex-valued perturbation and  $0 < \varepsilon \ll 1$ . Let us first address the situation when the perturbed potential is still Wadati type, i.e., it can be represented as  $y^2(x) + iy_x(x)$  for some  $y(x)$  which is real valued, but not necessarily antisymmetric. In this case the effect of the perturbation is expected to be merely quantitative, and families of stable nonlinear modes are expected to exist. The difference between  $y(x)$  and  $w(x)$  will only result in a slight deformation of solutions. However, if the perturbed potential does not belong to the Wadati class, then the effect of the perturbation becomes stronger. For this case we expect that stationary nonlinear modes predicted in our study will transform into “pseudomodes,” i.e., approximate solutions with propagation constants having small imaginary parts (of order of  $\varepsilon$ ). In the mathematical sense, those pseudomodes are not authentic solutions of the governing envelope equation. However, these objects are expected to be dynamically robust, i.e., to feature nearly stationary evolution for sufficiently long propagation distances. Therefore, they can still be regarded as meaningful physical entities, and their quasistable behavior is expected to be distinctively different from the authentically unstable propagation of linear waves. Some properties of such pseudomodes in a different class of complex potentials have been recently discussed in Ref. [39].

#### ACKNOWLEDGMENTS

The research was supported by the Priority 2030 Federal Academic Leadership Program.

- 
- [1] V. V. Konotop, J. Yang, and D. A. Zezyulin, Nonlinear waves in  $\mathcal{PT}$ -symmetric systems, *Rev. Mod. Phys.* **88**, 035002 (2016).
  - [2] V. Suchkov, A. A. Sukhorukov, J. Huang, S. V. Dmitriev, C. Lee, and Y. S. Kivshar, Nonlinear switching and solitons in  $\mathcal{PT}$ -symmetric photonic systems, *Laser Photon. Rev.* **10**, 177 (2016).
  - [3] L. Feng, R. El-Ganainy, and L. Ge, Non-Hermitian photonics based on parity-time symmetry, *Nat. Photonics* **11**, 752 (2017).
  - [4] R. El-Ganainy, K. G. Makris, M. Khajavikhan, Z. H. Musslimani, S. Rotter, and D. N. Christodoulides, Non-Hermitian physics and  $\mathcal{PT}$  symmetry, *Nat. Phys.* **14**, 11 (2018).
  - [5] Ş. K. Özdemir, S. Rotter, F. Nori, and L. Yang, Parity-time symmetry and exceptional points in photonics, *Nat. Mater.* **18**, 783 (2019).
  - [6] S. K. Gupta, Y. Zou, X. Zhu, M. Lu, L. Zhang, X. Liu, and Y. Chen, Parity-time symmetry in non-Hermitian complex optical media, *Adv. Mater.* **32**, 1903639 (2019).
  - [7] H. Nasari, G. G. Pyrialakos, D. N. Christodoulides, and M. Khajavikhan, Non-Hermitian topological photonics, *Opt. Mater. Express* **13**, 870 (2023).
  - [8] Y. Lumer, Y. Plotnik, M. C. Rechtsman, and M. Segev, Nonlinearly induced  $\mathcal{PT}$  transition in photonic systems, *Phys. Rev. Lett.* **111**, 263901 (2013).
  - [9] Y. Zhang, Z. Chen, B. Wu, T. Busch, and V. V. Konotop, Asymmetric loop spectra and unbroken phase protection due to nonlinearities in  $\mathcal{PT}$ -symmetric periodic potentials, *Phys. Rev. Lett.* **127**, 034101 (2021).
  - [10] I. V. Barashenkov and M. Gianfreda, An exactly solvable  $\mathcal{PT}$ -symmetric dimer from a Hamiltonian system of nonlinear oscillators with gain and loss, *J. Phys. A: Math. Theor.* **47**, 282001 (2014).
  - [11] I. V. Barashenkov, D. E. Pelinovsky, and P. Dubard, Dimer with gain and loss: Integrability and  $\mathcal{PT}$ -symmetry restoration, *J. Phys. A: Math. Theor.* **48**, 325201 (2015).
  - [12] I. V. Barashenkov, F. Smuts, and A. Chernyavsky, Integrability and trajectory confinement in  $\mathcal{PT}$ -symmetric waveguide arrays, *J. Phys. A: Math. Theor.* **56**, 165701 (2023).
  - [13] D. A. Zezyulin and V. V. Konotop, Nonlinear modes in finite-dimensional  $\mathcal{PT}$ -symmetric systems, *Phys. Rev. Lett.* **108**, 213906 (2012).



- [14] Z. Yan, Z. Wen, and C. Hang, Spatial solitons and stability in self-focusing and defocusing Kerr nonlinear media with generalized parity-time-symmetric Scarff-II potentials, *Phys. Rev. E* **92**, 022913 (2015).
- [15] Z. Yan, Z. Wen, and V. V. Konotop, Solitons in a nonlinear Schrödinger equation with  $\mathcal{PT}$ -symmetric potentials and inhomogeneous nonlinearity: Stability and excitation of nonlinear modes, *Phys. Rev. A* **92**, 023821 (2015).
- [16] Y. Chen and Z. Yan, Solitonic dynamics and excitations of the nonlinear Schrödinger equation with third-order dispersion in non-Hermitian  $\mathcal{PT}$ -symmetric potentials, *Sci. Rep.* **6**, 23478 (2016).
- [17] Y. Chen and Z. Yan, Stable parity-time-symmetric nonlinear modes and excitations in a derivative nonlinear Schrödinger equation, *Phys. Rev. E* **95**, 012205 (2017).
- [18] N. Saha and B. Roy, Solitons supported by competing nonlinearity, higher order dispersion and  $\mathcal{PT}$ -symmetric potential, *Phys. Lett. A* **384**, 126245 (2020).
- [19] M. Wadati, Construction of parity-time symmetric potential through the soliton theory, *J. Phys. Soc. Jpn.* **77**, 074005 (2008).
- [20] E. N. Tsoy, I. M. Allayarov, and F. Kh. Abdullaev, Stable localized modes in asymmetric waveguides with gain and loss, *Opt. Lett.* **39**, 4215 (2014).
- [21] V. V. Konotop and D. A. Zezyulin, Families of stationary modes in complex potentials, *Opt. Lett.* **39**, 5535 (2014).
- [22] J. Yang and S. Nixon, Stability of soliton families in nonlinear Schrödinger equations with non-parity-time-symmetric complex potentials, *Phys. Lett. A* **380**, 3803 (2016).
- [23] J. Yang, Analytical construction of soliton families in one- and two-dimensional nonlinear Schrödinger equations with nonparity-time-symmetric complex potentials, *Stud. Appl. Math.* **147**, 4 (2021).
- [24] F. C. Moreira and S. B. Cavalcanti, Optical solitons in a saturable nonlinear medium in the presence of an asymmetric complex potential, *J. Opt. Soc. Am. B* **37**, 3496 (2020).
- [25] D. A. Zezyulin, Continuous families of non-Hermitian surface solitons, *Opt. Lett.* **48**, 4773 (2023).
- [26] J. Yang, Symmetry breaking of solitons in one-dimensional parity-time-symmetric optical potentials, *Opt. Lett.* **39**, 5547 (2014).
- [27] S. Nixon and J. Yang, All-real spectra in optical systems with arbitrary gain-and-loss distributions, *Phys. Rev. A* **93**, 031802(R) (2016).
- [28] J. Yang, Classes of non-parity-time-symmetric optical potentials with exceptional-point-free phase transitions, *Opt. Lett.* **42**, 4067 (2017).
- [29] D. A. Zezyulin and V. V. Konotop, A universal form of localized complex potentials with spectral singularities, *New J. Phys.* **22**, 013057 (2020).
- [30] C. Hang, G. Gabadadze, and G. Huang, Realization of non- $\mathcal{PT}$ -symmetric optical potentials with all-real spectra in a coherent atomic system, *Phys. Rev. A* **95**, 023833 (2017).
- [31] L. D. Landau and E. M. Lifshitz, *Quantum Mechanics: Nonrelativistic Theory*, 2nd ed. (Pergamon, Oxford, 1965), p. 60.
- [32] V. E. Zakharov and A. B. Shabat, Exact theory of two-dimensional self-focusing and onedimensional self-modulation of waves in nonlinear media, *Zh. Eksp. Teor. Fiz.* **61**, 118 (1971) [*Sov. Phys.-JETP* **34**, 62 (1972)].
- [33] G. L. Lamb, *Elements of Soliton Theory* (Wiley, New York, 1980).
- [34] M. Klaus and J. K. Shaw, On the eigenvalues of Zakharov-Shabat systems, *SIAM J. Math. Anal.* **34**, 759 (2003).
- [35] R. M. Miura, Korteweg-de Vries equation and generalizations. I. A remarkable explicit nonlinear transformation, *J. Math. Phys.* **9**, 1202 (1968).
- [36] D. Ananikian and T. Bergeman, Gross-Pitaevskii equation for Bose particles in a double-well potential: Two-mode models and beyond, *Phys. Rev. A* **73**, 013604 (2006).
- [37] A. Sacchetti, Universal critical power for nonlinear Schrödinger equations with a symmetric double well potential, *Phys. Rev. Lett.* **103**, 194101 (2009).
- [38] Z. H. Musslimani, K. G. Makris, R. El Ganainy, and D. N. Christodoulides, Optical solitons in  $\mathcal{PT}$ -periodic potentials, *Phys. Rev. Lett.* **100**, 030402 (2008).
- [39] D. A. Zezyulin, A. O. Slobodyanyuk, and G. L. Alfimov, On nonexistence of continuous families of stationary nonlinear modes for a class of complex potentials, *Stud. Appl. Math.* **148**, 99 (2022).